

# Resist evaluation for proton beam writing, Ni mold fabrication and nano-replication

Y. H. Wang, P. Malar & J. A. van Kan

**Microsystem Technologies**  
Micro- and Nanosystems Information  
Storage and Processing Systems

ISSN 0946-7076  
Volume 20  
Combined 10-11


Microsyst Technol (2014) 20:2079-2088  
DOI 10.1007/s00542-014-2070-6

542 Research Journal

# Microsystem Technologies

20  
10-11

Micro- and Nanosystems  
Information Storage  
and Processing Systems



Editors-in-Chief:  
B. Michel  
B. Bhushan

Volume 20 · Numbers 10-11 · October 2014

**Special Issue: The 10th International Workshop on High Aspect Ratio Micro and Nanosystem Technologies (HARMNST), Berlin, April 21-24, 2013**

EDITORIAL  
Editorial special issue HARMNST 2013  
J. Mohr · J. Göttert · B. Michel 1771

TECHNICAL PAPERS  
Nanoimprint lithography and micro-embossing in LIGA technology: similarities and differences  
H. Schiff 1773  
SAM meets MEMS: reliable fabrication of stable Au-patterns embedded in PDMS using dry peel-off process  
I. Byun · A.W. Coleman · B. Kim 1783  
ViPER: simulation software for high aspect ratio plasma etching of silicon  
V. Ishchuk · B.E. Volland · I.W. Rangelow 1791

High-aspect-ratio nanoporous membranes made by reactive ion etching and e-beam and interference lithography  
R. Divan · O.V. Makarova · S. Skoog · R. Narayan · A.V. Sumant · C.-M. Tang · N. Moldovan 1797  
IR-drying of photoresists: experimental and theoretical consideration of drying kinetics of mono- and multi-layered coatings  
M. Schönfeld · S. Schubert · J. Saupe · J. Grimm 1803  
Large tuning ratio high aspect ratio variable capacitors using leveraged bending  
S. Achenbach · D.T. Haluzan · D.M. Klymyshyn · M. Börner · J. Mohr 1807  
Arrays of high-aspect ratio microchannels for high-throughput isolation of circulating tumor cells (CTCs)  
M.L. Hupert · J.M. Jackson · H. Wang · M.A. Witek · J. Kamande · M.L. Milowsky · Y.E. Whang · S.A. Soper 1815

(Continuation on cover page IV)

20 (10-11) 1771-2008 (2014)

**Your article is protected by copyright and all rights are held exclusively by Springer-Verlag Berlin Heidelberg. This e-offprint is for personal use only and shall not be self-archived in electronic repositories. If you wish to self-archive your article, please use the accepted manuscript version for posting on your own website. You may further deposit the accepted manuscript version in any repository, provided it is only made publicly available 12 months after official publication or later and provided acknowledgement is given to the original source of publication and a link is inserted to the published article on Springer's website. The link must be accompanied by the following text: "The final publication is available at [link.springer.com](http://link.springer.com)".**

# Resist evaluation for proton beam writing, Ni mold fabrication and nano-replication

Y. H. Wang · P. Malar · J. A. van Kan

Received: 5 June 2013 / Accepted: 7 January 2014 / Published online: 22 January 2014  
© Springer-Verlag Berlin Heidelberg 2014

**Abstract** Proton beam writing (PBW) is a new direct-write technique which has shown great potential to fabricate structures down to 20 nm level in resist material. Protons can be accelerated up to a high energy (3.5 MeV) at Centre for Ion Beam Applications. Because the mass of a proton is much larger than the mass of an electron ( $m_p:m_e = 1,800:1$ ), the energy of the secondary electrons is very small compared with secondary electrons generated by electron beam lithography. Therefore, a proton will travel along a straight path into resist and secondary electrons will only expose the resist within several nanometers around the path of the proton. PBW is capable of fabricating structures with very straight, vertical and smooth side-walls without proximity effect. This is very important when combining PBW with Ni electroplating and nanoimprinting as well as injection molding. High quality Ni molds with smooth and vertical side walls are critical in nanoimprint lithography and injection molding. In our experiments, several new resists including AR-P 3250, a mixture of AR-P 3250 and AR 300-12, and ma-N 2401 are tested with PBW for the production of high aspect ratio Ni molds and thermoplastic replication with these molds. High aspect ratio structures (up to 7) are fabricated at a width of 500 nm in Ni molds. The structures are transferred to plastic via nanoimprinting and injection molding.

## 1 Introduction

Proton beams have been used in lithography for almost 30 years. In early experiments Adesida (1985) and Brenner et al. (1990) used low (200 keV) and high (8 MeV) energetic proton beams, respectively for masked irradiation of poly(methyl methacrylate) (PMMA) resist materials. In this early work Adesida produced rather rough sub-100 nm features, whereas Brenner et al. produced very high aspect ratio structures featuring lateral dimensions of tens of microns. More recently proton beam writing (PBW) was introduced as a direct-write technique, developed in Centre for Ion Beam Applications (CIBA), National University of Singapore (Springham et al. 1997; Watt et al. 2003). At CIBA, there is a Singletron accelerator which can accelerate protons up to an energy of 3.5 MeV. This direct-write lithographic technique employs a focused MeV proton beam to pattern suitable resists (van Kan et al. 1999, 2008). PBW has several advantages over e-beam lithography. Firstly, proximity effects in PBW are practically absent, because the energy of secondary electrons is typically eVs which leads to an energy density distribution around the proton track of only a few nanometers (Udalagama et al. 2007). Secondly, PBW is capable of fabricating high aspect ratio sub 100 nm structures with vertical and smooth side walls since a MeV proton can penetrate to very large depth in resist (van Kan et al. 2000, 2003; Bier-sack and Haggmark 1980; Simicic et al. 2005; Rajta et al. 2007). Thirdly, PBW has a 100 fold higher sensitivity than e-beam lithography in the same resist material (van Kan et al. 2007). At CIBA, PBW has been demonstrated as a fast single step direct write technique for fabrication of sub-30 nm high aspect ratio structures in resists with less than 3 nm side wall roughness (van Kan et al. 2003). Nowadays protons can be focused down to  $19.0 \times 29.9$  nm

Y. H. Wang · J. A. van Kan (✉)  
Department of Physics, Center for Ion Beam Applications  
(CIBA), National University of Singapore, 2 Science Drive 3,  
Singapore 117542, Singapore  
e-mail: phyjavk@nus.edu.sg

P. Malar  
Research Institute, SRM University, Kattankulathur,  
Chennai 603203, India

at CIBA (van Kan et al. 2012) and 22 nm lines with a high aspect ratio have been fabricated in hydrogen silsesquioxane (HSQ) (van Kan et al. 2006).

PBW has many advantages and already achieves some remarkable results, but there is still a long way to go before PBW can be used as a high throughput tool. However, in the rapid development of micro- and nanotechnology, the demand for low cost high-throughput technologies of fabricating micro- and nanometer scale structures is increasing. To fully utilize the strong points of PBW integration with mass replication techniques should be explored. There are many techniques such as nanoimprinting, injection molding and PDMS casting which enable low cost and high throughput replication of polymer structures. To employ these techniques, we have fabricated Ni molds through PBW and Ni electroplating. At CIBA, Ni mold with details down to 100 nm wide and 2  $\mu\text{m}$  tall walls have been fabricated by PBW and electroplating using positive PMMA resist (Ansari et al. 2004). In order to expand the applications of Ni molds in mass replication techniques, it is very important to investigate new resist materials especially negative resist materials which are suitable for the combination of PBW and electroplating. Ni molds have been used in many application areas, such as advanced printed circuit board (Lee et al. 2011), polymer microlens replication (Dutta et al. 2007) and some other optical devices (Oh

et al. 2011). However, most of the applications are either based on high aspect ratio (can be over 20) features in Ni molds with large structure sizes (several microns) (Lee et al. 2011) or feature high resolution (sub-100 nm) Ni molds with low aspect ratio (typically  $<2$ ) (Oh et al. 2011). Ni molds with high aspect ratio and high resolution structures are still hard to achieve. Here we present the results on ARP resist, allowing us to fabricate high aspect ratio nano structures.

## 2 Resist materials for PBW and Ni electroplating

Many resist materials have already been tested with PBW (van Kan et al. 1999, 2007). Among these resist materials, PMMA, SU-8 and HSQ are the most often used resist materials in PBW and sub-60 nm details with high aspect ratio have been demonstrated (van Kan et al. 2000, 2006). PMMA is a good positive photoresist which can be used to fabricate Ni mold in a wide range of thicknesses. Up to now thick negative resist materials are a challenge in combination with PBW and Ni electroplating; SU-8 is negative photoresist which can't be easily removed after PBW and Ni electroplating and is therefore not suitable for Ni mold fabrication. HSQ is also a negative photoresist having a very high resolution, but the thickness of HSQ is limited

**Table 1** Current status and dose requirements in PBW

| Resist                                 | Type     | Dose needed (nC/mm <sup>2</sup> ) | Smallest feature written                        |
|--|----------|-----------------------------------|---|
| PMMA (van Kan et al. 1999)             | Positive | 80–150                            | 20–30 nm  |
| SU-8 (van Kan et al. 2003)             | Negative | 30                                | 60 nm   |
| HSQ (Yao et al. 2014)                  | Negative | 30                                | 19 nm   |
| PMGI (van Kan et al. 1999)             | Positive | 150                               | 1.5 $\mu\text{m}$                               |
| WL-7154 (van Kan et al. 2011)          | Negative | 4–8                               | 260 nm  |
| TiO <sub>2</sub> (van Kan et al. 2007) | Negative | 8,000                             | 5 $\mu\text{m}$                                 |
| Si (Teo et al. 2004)                   | Negative | 80,000                            | 15 nm tip<br>(implanted in channeling geometry) |
| TADep (Valamontes et al. 2008)         | Negative | 125–238                           | 110 nm  |
| ma-N 2401                              | Negative | 40                                | 60 nm   |
| ma-N 2410 (van Kan et al. 2011)        | Negative | 70–200                            | 250 nm  |
| AR-P 3250                              | Negative | 30–50                             | 330 nm  |
| AR-P 3250: AR 300-12 = 1:3             | Negative | 50                                | 120 nm  |
| KMPR (Ynsa et al. 2011)                | Negative | 140                               | 1 $\mu\text{m}$                                 |
| ma-P 1275 HV (Liu et al. 2010)         | Negative | 20                                | 10 $\mu\text{m}$                                |
| Diaplate (Gonin et al. 2004)           | Negative | 10                                | 10 $\mu\text{m}$                                |
| PADC (CR-39) (Rajta et al. 2003, 2005) | Positive | 600                               | 5 $\mu\text{m}$                                 |
| Forturan (Rajta et al. 2003)           | Positive | 1                                 | 3 $\mu\text{m}$                                 |
| ma-N 440 (Menzel et al. 2007)          | Negative | 200                               | 400 nm  |
| GaAs (Mistry et al. 2007)              | Negative | 100,000                           | 12 $\mu\text{m}$                                |

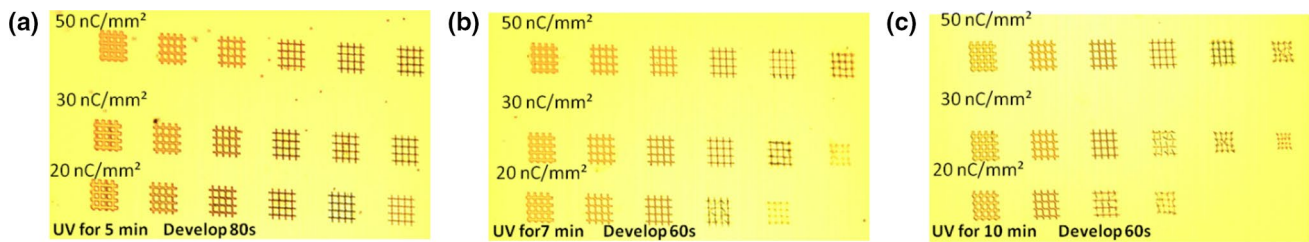


**Fig. 1** Three ARP 3250 samples used to optimize the dose of 1 MeV protons, UV exposure, and development time

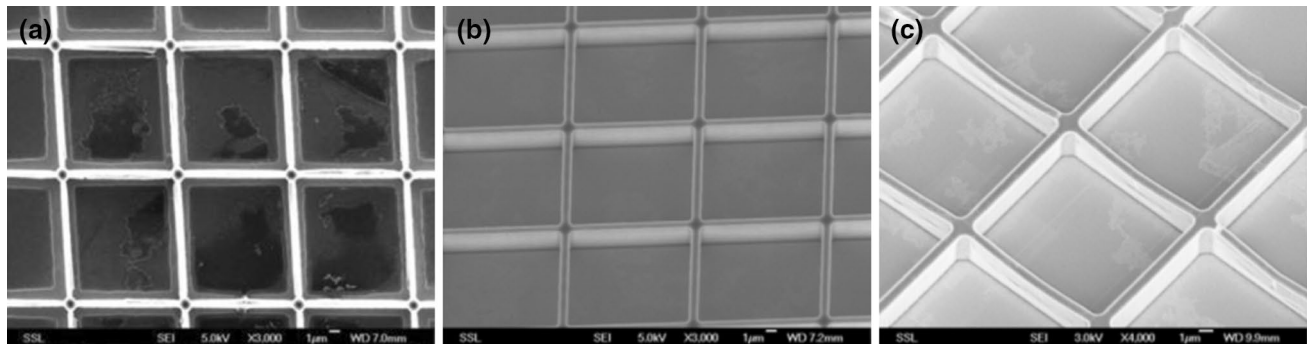


**Fig. 2** SEM image of grids **a** 800 nm wide and 1  $\mu\text{m}$  high grid (1 MeV protons, 5 min UV, 80 s development); **b** 800 nm wide and 4  $\mu\text{m}$  high grid (1 MeV protons, 7 min UV, 60 s development); **c** 800 nm wide grid (1 MeV protons, 10 min UV, 60 s development)

to sub-micron thickness. In Table 1, a summary of resists compatible with PBW is presented. In this research, three new resist materials were tested including AR-P 3250, a mixture of AR-P 3250 and AR 300-12, and ma-N 2401.

## 2.1 AR-P 3250

AR-P (All Resist GmbH) is a relatively high sensitive resist to UV (i-line 365 nm) (Dhima et al. 2011). In AR-P 3200 series, AR-P 3250 is designed for thick layers up to several  $\mu\text{m}$ . AR-P 3250 is a very interesting resist material since it shows positive resist behavior under UV exposure and negative resist behavior when exposed to protons. A contrast value around 2.0 was measured in PBW employing relatively large structures (Malar et al. 2012). In the process of PBW, the molecular chains of AR-P 3250 cross link; while through UV exposure, the chains are scissioned (Wang et al. 2013). In the process of UV exposure some of the molecular chains that have been crosslinked via proton exposure are broken, therefore the exposure dose of UV should be well controlled.

In the experiments presented here, a Si wafer was pre coated with Au and Cr followed by a bake at 200  $^{\circ}\text{C}$  for 30 min to remove any moist, then a layer of AR-P 3250 was spincoated to yield a layer of 3.5  $\mu\text{m}$  thickness. The resist was exposed with 1 or 2 MeV protons and exposure doses of 20 to 200  $\text{nC}/\text{mm}^2$ , followed by a flood UV exposure

(365 nm using a 100 W lamp) and development in AR 300-26 developer (1:1 diluted with DI water).

To fabricate small structures with AR-P 3250, a dose optimization was performed. As can be seen from Fig. 1, the structures were written with a 1 MeV proton beam at a dose of 20, 30 and 50  $\text{nC}/\text{mm}^2$  in a 4  $\mu\text{m}$  thick resist layer. Next the samples were exposed with UV. The designed width of the structure is 5  $\mu\text{m}$ , 3  $\mu\text{m}$ , 2  $\mu\text{m}$ , 800 nm, 500 nm and 340 nm from left to right. As can be seen from Fig. 1, the smaller structures are most affected by the UV exposure. UV exposure counteracts the cross linking by the proton irradiation, as a result small features exposed by the proton beam will become soft and are therefore not hard enough to remain standing or are removed completely during development. A higher proton dose will guarantee enough strength in the high aspect ratio structures i.e. a dose of 50  $\text{nC}/\text{mm}^2$  or more is typically enough to cross-link the resist. Figure 2 shows SEM images of the structures in Fig. 1 with 50  $\text{nC}/\text{mm}^2$  proton dose, different UV exposure time and different development time. As can be seen from Fig. 2a, a 5 min UV exposure and development for 80 s results in a structure height of 1  $\mu\text{m}$  or 25 % of the original resist thickness and relatively wide lines. This implies that the development time is too long and the UV exposure dose is not enough. Longer UV exposure time can ensure proper resist development and at the same time reduces the development time which protects the proton



beam written structures. Figure 2b shows structures which were exposed by UV for 7 min and developed for 60 s. The structure features 800 nm wide and 4  $\mu\text{m}$  tall grid bars with smooth and vertical side walls, free from unwanted resist. For even longer UV exposure, the grids fabricated by PBW are affected; An exposure of 10 min counteracts the cross linking by the proton irradiation resulting in weakening of the resist as shown in Fig. 2c. For an exposure of 4  $\mu\text{m}$

thick resist and a proton dose of 50  $\text{nC}/\text{mm}^2$  at 1 MeV the optimum UV exposure time is 7 min and development time 60 s. Figure 3 shows the normalized contrast curve (height of the resist as a function of exposure dose) for AR-P 3250 exposed to 1 MeV protons followed by UV exposure and chemical development. The contrast curve was measured with the structures at a width of 500 nm. Here the contrast is defined as  $\gamma = 1/[\log(Df) - \log(Di)]$  where  $Df$  is the

**Fig. 3** Contrast curve of AR-P 3250, obtained for 500 nm wide structures in a 4  $\mu\text{m}$  coated resist layer using 1 MeV protons, 7 min UV and 60 s development

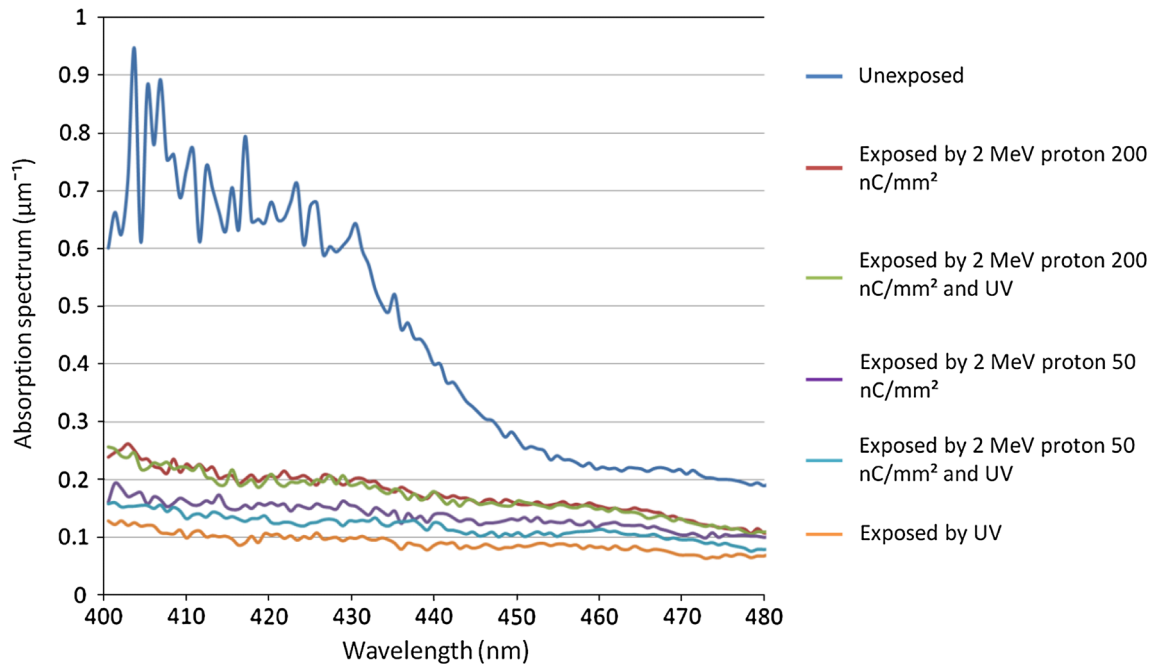
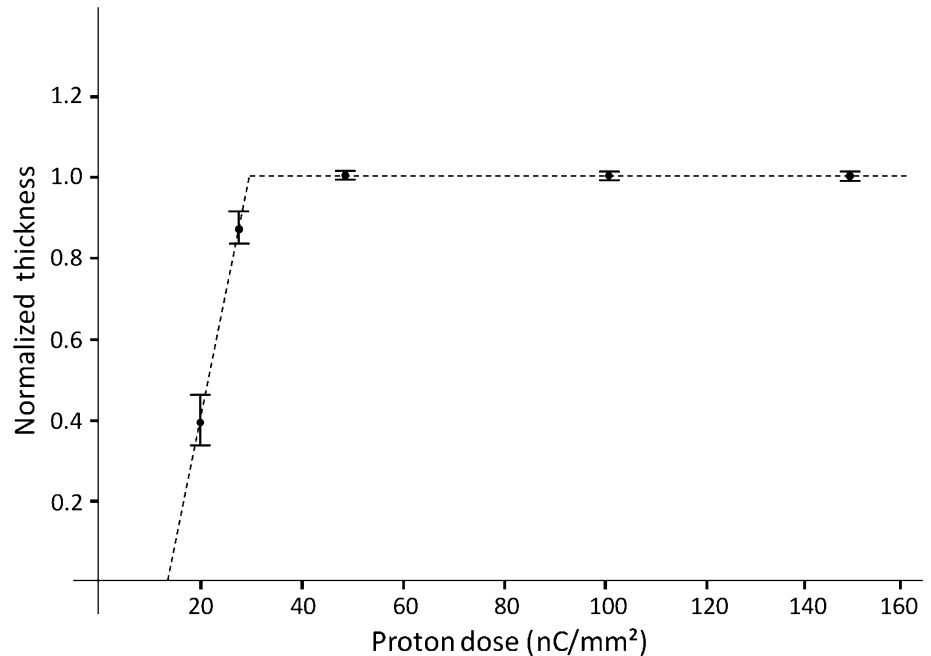


**Fig. 4** Absorption spectrum of AR-P 3250 exposed to 2 MeV protons and 10 min UV exposure

dose at which the resist is fully insoluble and  $D_i$  the dose where the resist becomes insoluble in the developer (Zheng 2005). The measured contrast value is  $\gamma = 3.5 \pm 0.5$  which is higher than previously reported. This is due to different sizes of the structures. The contrast reported earlier was measured using large structures (of  $10 \times 10 \mu\text{m}^2$ ) (Malar et al. 2012), which are much more porous than the 500 nm structures used here. A relatively low proton dose is enough for large porous structures, however, a higher dose is needed to support high aspect ratio nano structures.

In order to characterize AR-P resist in more detail, the absorption of AR-P 3250 was measured as a function of wavelength using a DH-2000 BAL from 330 to 2,000 nm and a spectrometer (QE 65000) to analyze the light intensity ( $\lambda > 400 \text{ nm}$ ). AR-P 3250 was spincoated to yield a layer of  $5 \mu\text{m}$  thick. The resist was exposed by 2 MeV protons using 50 and  $200 \text{ nC/mm}^2$ . This corresponds to an equivalent dose of 30 and  $120 \text{ nC/mm}^2$  for a 1 MeV proton exposure, corrected for the stopping power (Ziegler 1999). The absorption was measured for non exposed and proton exposed AR-P 3250 resist. To establish the effect of the UV exposure on the proton exposed areas all the structures were exposed to 10 min UV (a thick layer requires a longer UV exposure to compensate absorption) and the absorption of the AR-P 3250 was measured again. Figure 4 shows the absorption spectra of AR-P 3250 resist under different conditions, as can be seen resist exposed to protons has an absorption between the absorption of plain resist and standard UV exposed resist, an increased proton dose, results in an increased absorption. Since unexposed AR-P resist has high absorption and is not affected by the development it is expected that proton exposed resist with a

higher absorption is able to withstand the development procedure. This explains the fact that AR-P 3250 is a negative resist under proton exposure followed by UV exposure. As can be seen from Fig. 4, after proton exposure at  $50 \text{ nC/mm}^2$  followed by UV exposure the absorption is reduced and becomes closer to the standard UV exposed resist. This observation implies that UV exposure changes the properties of proton exposed resist and brings its characteristics closer to standard UV exposed resist. After development a height of 3 and  $5 \mu\text{m}$  for the resist exposed with 50 and  $200 \text{ nC/mm}^2$  protons is observed, respectively. Since 2 MeV protons at a dose of  $50 \text{ nC/mm}^2$  have an equivalent dose of  $30 \text{ nC/mm}^2$  at 1 MeV, the observed heights match the contrast curve presented in Fig. 3.

With optimization using 1 MeV protons at  $50 \text{ nC/mm}^2$  and 6 min UV exposure and 60 s development, 330 nm wide lines forming a grid of AR-P 3250 standing  $3.5 \mu\text{m}$

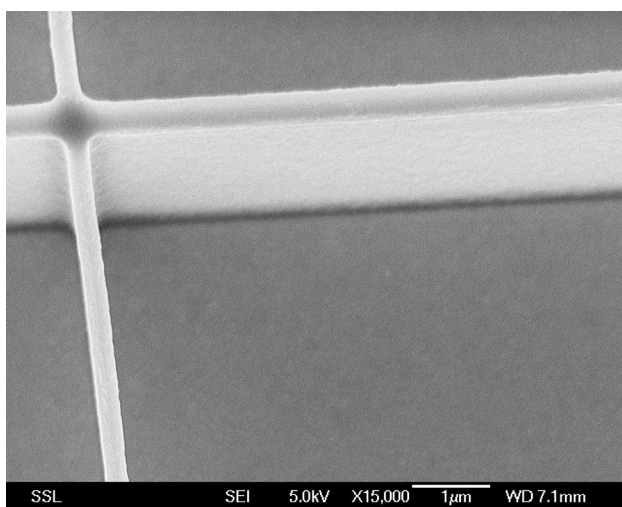


**Fig. 5** 330 nm wide line written in  $3.5 \mu\text{m}$  thick AR-P 3250 via 1 MeV Proton beam writing, 6 min UV exposure and 60 s development

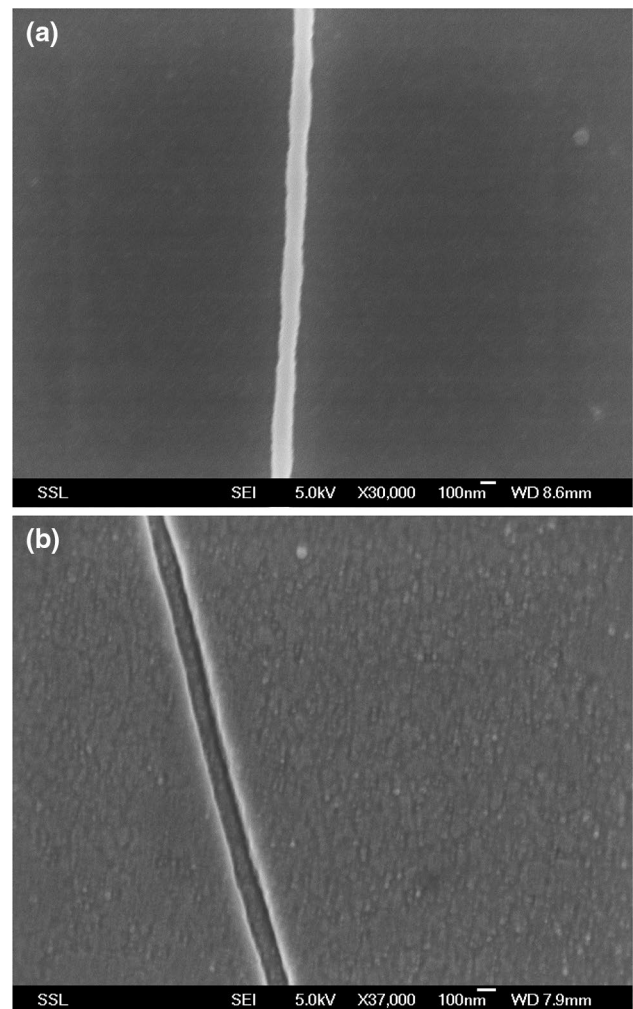


**Fig. 6 a** 120 nm wide line in mixture (AR-P 3250: AR 300-12 = 1:3) written by 1 MeV proton beam **b** 120 nm wide and 280 nm deep groove in Ni

tall are fabricated (Fig. 5), corresponding to an aspect ratio of more than 10. As can be seen, smooth and vertical side walls can be achieved by PBW. In fact, even smaller features down to 200 nm in 4  $\mu\text{m}$  thick AR-P 3250 can be fabricated. However, such a high aspect ratio (20) leads to resist collapse.

## 2.2 Mixture of AR-P 3250 and AR 300-12

Since AR-P 3250 exhibits very good results based on PBW and electroplating, it is good to make full use of this resist. AR-P 3250 can be coated reaching layer thicknesses of 3–11  $\mu\text{m}$ , however sometimes thinner layers of photoresist are required. A thin layer of AR-P resist can be obtained by mixing AR-P 3250 and AR 300-12 (All Resist GmbH). In our experiment, AR-P 3250 and AR 300-12 were mixed with a ratio of 1:3 (Mixture with a different ratio gives different thickness at specific spincoated speed). The mixture has similar property with AR-P 3250. Before resist coating, a Si wafer was coated with Au and Cr and baked at 200 °C for 30 s to remove any moist. Then, the mixture was spincoated at 4,000 rpm for 30 s followed by a pre bake at 95 °C for 30 s. This yielded a layer thickness of 280 nm. A 1 MeV proton beam focused down to  $100 \times 150$  nm was used to pattern the resist. Details down to 120 nm have been fabricated at a dose of 50 nC/mm<sup>2</sup> by PBW and UV exposure for 1 min, followed by development for 20 s (shown in Fig. 6a). The aspect ratio of the line is about 2.5. To perform electroplating, a layer of 6 nm Ti was coated to act as a secondary seed layer for electroplating. Electroplating was performed in a Technotrans RD 50 plating machine at a rate of 104 A/dm<sup>2</sup> for about 42 h, yielding a total thickness of 0.5 mm. After electroplating, the Si wafer and Ni mold were separated by ultrasonic and acetone cleaning for 20 min. As can be seen in Fig. 6b, the structures were accurately transferred to Ni and all the resist in the grooves was completely removed by the acetone, featuring 120 nm grooves. As a result, the mixture resist is a suitable resist for higher resolution structures in Ni mold fabrication.

## 2.3 ma-N 2401

ma-N (Micro Resist Technology GMBH) is a negative tone photoresist series designed for the use in micro- and nano-electronics. Conventional negative tone resists typically have poor resolution. ma-N 2400 was developed to allow high tolerance in resist process control and achieve high resolution; 80 nm line and space patterns have been obtained via electron beam lithography in ma-N 2400 at 20 kV (Voigt et al. 1999). Menzel et al. (2007) have shown Ni grids faithfully replicated from PBW fabricated maN-440 resist structures. ma-N 2410 was also tested with

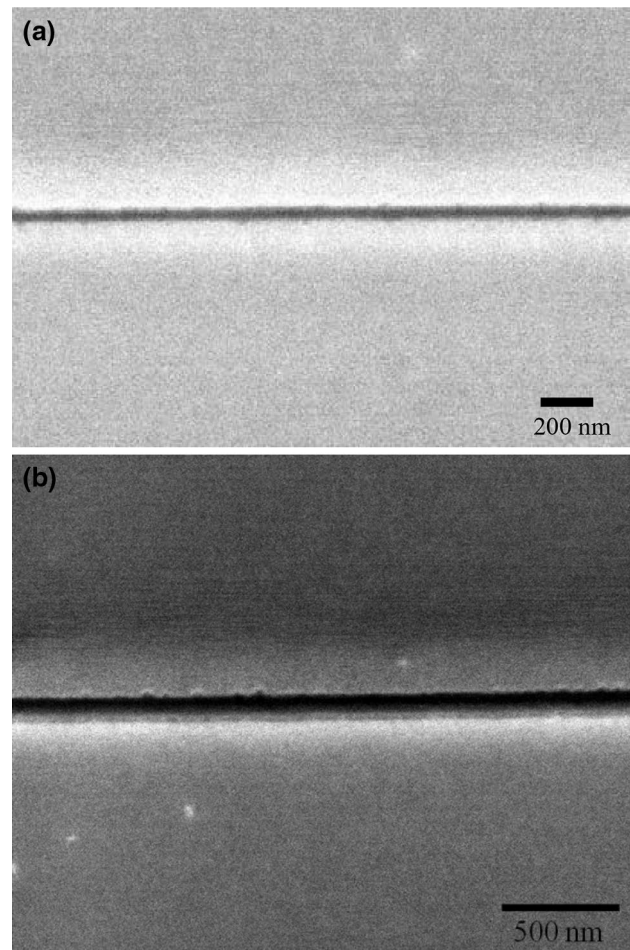


**Fig. 7** a 60 nm line in 100 nm thick ma-N 2401 via 1 MeV proton beam writing (b) 100 nm line in 100 nm thick ma-N 2401 (the sample was tilted for 30°)

PBW at CIBA (van Kan et al. 2011), and 500 nm details in 1  $\mu\text{m}$  thick resist were fabricated with 1 MeV proton and accurately transferred to Ni mold. ma-N 2401 also has been used in PBW and electroplating. Ni channels down to 800 nm wide and 110 nm high were achieved (Liu et al. 2013). Here we use ma-N 2401 in combination with PBW, pursuing higher resolution. Au and Cr were first coated on Si wafer followed by a bake at 200 °C for 30 min to remove any moist. ma-N 2401 was spincoated at 3,000 rpm for 30 s yielding a layer of 100 nm. The ma-N 2401 layer was exposed with 1 MeV proton beam at a dose of 40 nC/mm<sup>2</sup>, then development in ma-D 525 for 13 s, rinsed with DI water for 2 min and air dried. As can be seen from Fig. 7a, a 60 nm line in 100 nm thick ma-N 2401 was fabricated with PBW. Figure 7b shows the side wall of the 100 nm wide line in ma-N 2401. After electroplating, ultrasonic and acetone cleaning were used to remove resist. The resist was stuck in Ni because the size of the structure was possibly too small.



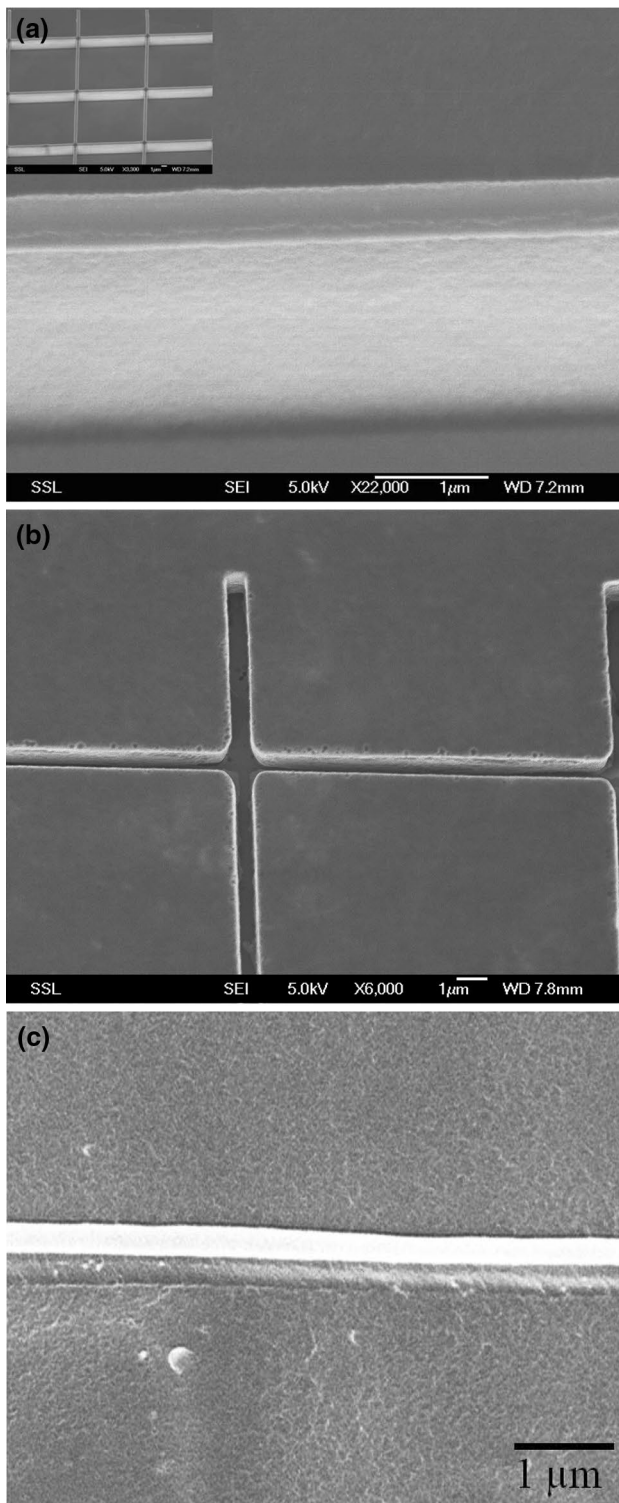


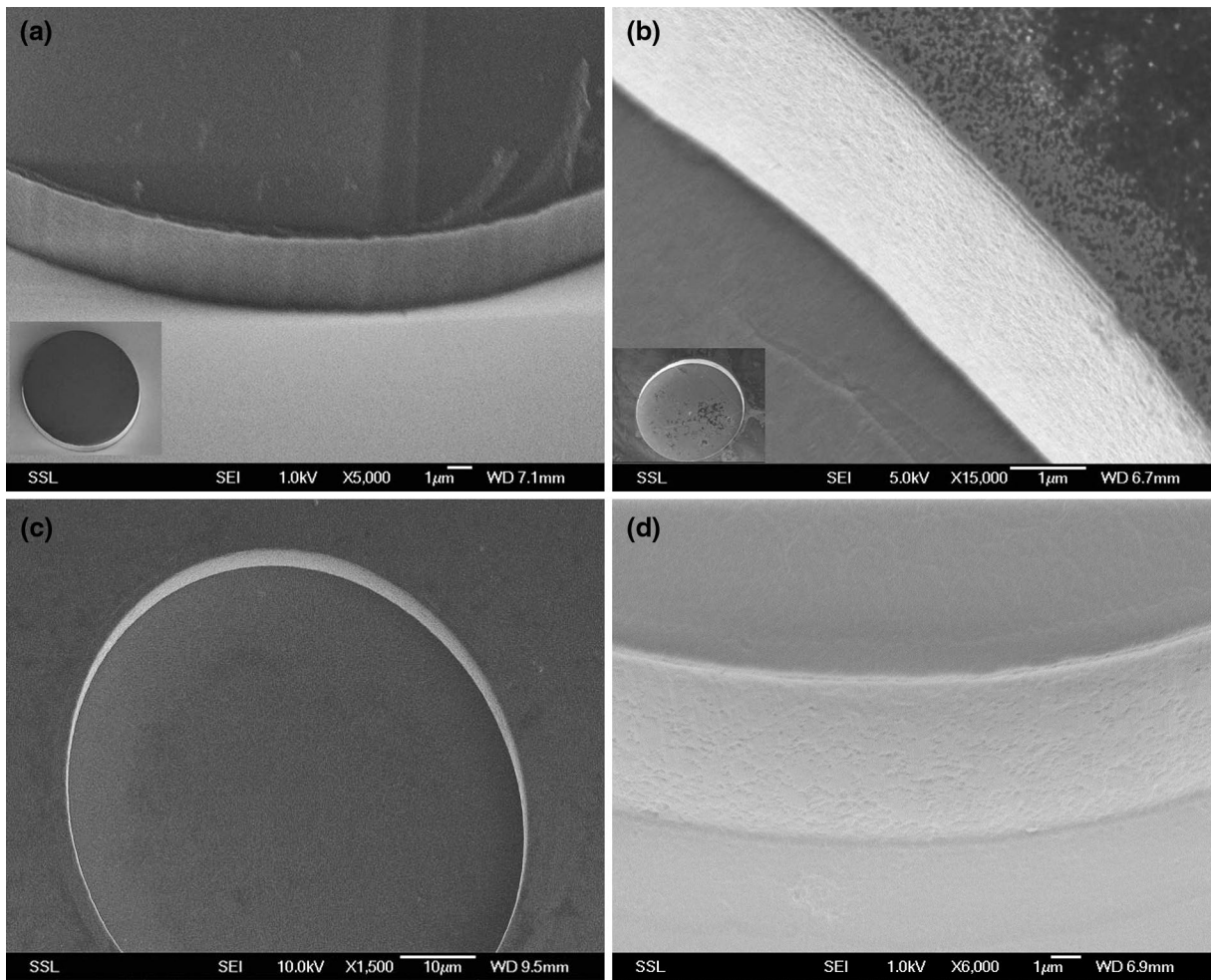
**Fig. 8** **a** 500 nm wide and 4  $\mu\text{m}$  high line in AR-P 3250 **b** 500 nm wide and 4  $\mu\text{m}$  deep grooves in Ni **c** 500 nm wide and 4  $\mu\text{m}$  high ridge in spincoated PMMA obtained via nanoimprinting

### 3 Ni molds for nanoimprinting and injection molding

Ni mold fabricated with PBW and electroplating has already proven to be a remarkable approach in nanoimprinting. Details down to 100 nm wide and 2  $\mu\text{m}$  deep channels have been imprinted on PMMA with Ni mold fabricated by PBW of PMMA resist and electroplating (Ansari et al. 2004). In order to expand molding applications, Ni molds were fabricated with negative resists. Here we discuss the Ni molds fabricated with AR-P 3250, the mixture resist (AR-P 3250: AR 300-12 = 1: 3) and ma-N 2410 in nanoimprinting and injection molding experiments.

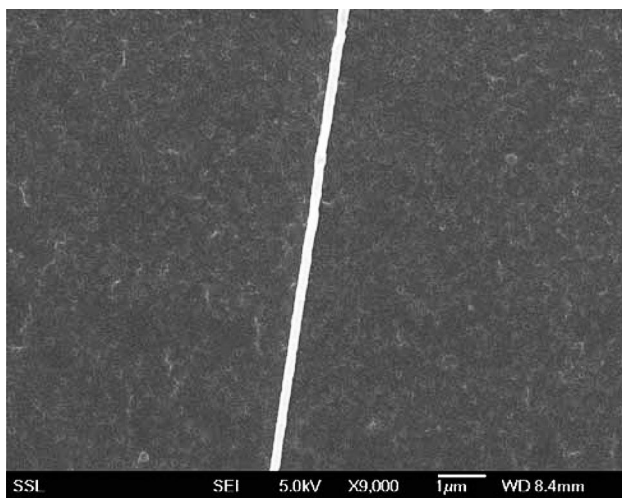
With AR-P 3250, we have used 500 nm wide lines for Ni electroplating. To perform electroplating, a 6 nm Ti layer was coated on the surface of the resist sample as a secondary seed layer using filtered cathodic arc vacuum deposition method ( $10^{-5}$  mbar). Electroplating was performed in a Technotrans RD 50 plating machine at a rate of 260.4 A/dm<sup>2</sup> for about 33.5 h, yielding a total thickness of 1.0  $\mu\text{m}$ . After removing Si and resist, a pure Ni mold is fabricated. Figure 8a shows the 500 nm wide line in AR-P 3250. Figure 8b shows the Ni grooves down to 500 nm, 4  $\mu\text{m}$  deep. As can be seen, AR-P 3250 resist patterns were accurately transferred to Ni and the resist was completely removed with acetone. The result indicates that PBW patterned AR-P 3250 resist structures are promising to make high quality Ni molds with high aspect ratio features at the micro- and nano-scale. This Ni mold sample was used in nanoimprinting. Prior to nanoimprinting a 5  $\mu\text{m}$  thick PMMA resist 950,000 MW (11 wt%) in anisole was spincoated on a Si wafer. Then the sample was pre baked at 180  $^{\circ}\text{C}$  for 90 s to completely remove any solvent. Nanoimprinting was carried out with a commercial nanoimprinter (Obducat Technologies AB, NIL-2-PL 2.5" nanoimprinter). The mold shown in Fig. 8b was tested in the nanoimprinter. The imprinting cycle consists of 20 s at 100  $^{\circ}\text{C}$  and 20 bar, followed by 30 s at 120  $^{\circ}\text{C}$  and 30 bar. The pressure was released after cooling just below 80  $^{\circ}\text{C}$ . Figure 8c shows the SEM image of the PMMA ridge imprinted on the spincoated PMMA. The width of the ridge is 500 nm, and the height is about 3.5  $\mu\text{m}$  which matches the dimension in the Ni mold. As can be seen, the side wall of the structure is also very smooth.

Figure 9a shows a tilted SEM image of a 60  $\mu\text{m}$  diameter pillar on 10  $\mu\text{m}$  thick AR-P 3250. The PBW patterned pillar in the resist also exhibits a very smooth and straight side wall. Figure 9b shows the electroplated Ni holes from the patterned pillar in the resist. The smooth and straight features of the pillar have been well replicated into the metal



**Fig. 9** a SEM image of proton beam written 10 μm high AR-P 3250 pillar b SEM image of Ni mold fabricated from AR-P 3250 (10 μm deep) c 11 μm deep hole in Ni fabricated with resist AR-P 3250 d

11 μm high pillar imprinted on PMMA sheet exhibiting vertical and smooth sidewall



**Fig. 10** SEM image of 120 nm wide and 280 nm high line imprinted on spincoated PMMA

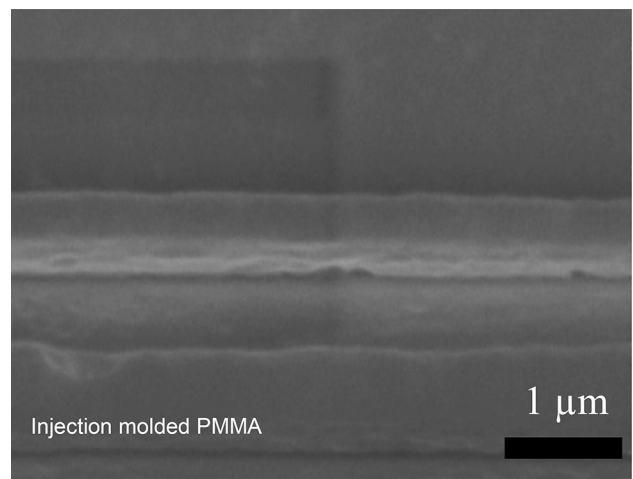


**Fig. 11** SEM image of injection molded PMMA featuring 500 nm wide and 1 μm high line

as a 10  $\mu\text{m}$  deep hole. Figure 9c shows a 11  $\mu\text{m}$  deep Ni hole which is also electroplated with AR-P 3250 as resist. Electroplating was performed at a rate of 260.4 A/dm<sup>2</sup> for 200 min reaching 100  $\mu\text{m}$ , followed by 520.8 A/dm<sup>2</sup> for 40 h, yielding a total thickness of 2.5  $\mu\text{m}$ . As can be seen, the side wall of the hole is very smooth. Next the Ni mold with 11  $\mu\text{m}$  deep hole was tested with Obducat Technologies AB, NIL-2-PL 2.5" nanoimprinter. The structures were imprinted onto a piece of 850  $\mu\text{m}$  thick PMMA sheet. The imprinting cycle consists of 20 s at 100 °C and 20 bar, followed by 240 s at 120 °C and 30 bar. The pressure was released after cooling just below 80 °C. Figure 9d shows the side wall of the pillar in the PMMA sheet. As can be seen, the side wall is as smooth as the original Ni mold.

A Ni mold fabricated with the mixture resist (AR-P 3250: AR 300-12 = 1: 3) was also used in the same nanoimprinter. The imprinting cycle consists of: 20 s at 100 °C and 20 bar, followed by 15 s at 120 °C and 30 bar. The pressure was released after cooling just below 80 °C. An electron micrograph of the imprinted line is shown in Fig. 10. The replicated pattern featuring 120 nm wide and 280 nm high line was accurately transferred from the Ni mold to 5  $\mu\text{m}$  thick spincoated PMMA.

ma-N 2410 is a negative resist to PBW. 500 nm grooves with 1  $\mu\text{m}$  depth has been fabricated in Ni combined with PBW (Wang et al. 2013). This Ni mold was used in injection molding—Battenfeld 5 TON Micro Molding Machine. Plastic PMMA was used in this process. The mold temperature is 100 °C and the injection speed is 700 mm/s. Figure 11 shows the molded PMMA featuring a 500 nm wide and 1  $\mu\text{m}$  tall line (2 aspect ratio). As can be seen, the structure was accurately transferred to PMMA from the Ni mold using injection molding.

#### 4 Conclusions

In our experiment, we present a new negative resist AR-P 3250 for PBW and Ni electroplating which is useful for fabricating high quality Ni molds with high aspect ratio and high resolution structures. Previously only positive resist were successfully transferred into Ni molds in combination with PBW. This new resist opens up easy fabrication of high aspect ratio and high resolution Ni molds. In addition, an improved contrast ( $\gamma = 3.5$ ) was measured for small structures in AR-P 3250. The resist absorption behaviour of AR-P 3250 exposed by PBW and UV was also investigated through absorption measurements. 330 nm wide lines in 3.5  $\mu\text{m}$  thick AR-P 3250 were fabricated with 1 MeV proton exhibiting vertical and smooth sidewalls. AR-P 3250 structures were well transferred to Ni via electroplating. Grooves with a high aspect ratio up to 7 in Ni were realized. Resist in the grooves was completely removed by

acetone. Nanoimprinting with this Ni mold also succeeded to replicate 500 nm wide and 3.5  $\mu\text{m}$  high lines in a spin-coated PMMA layer. An 11  $\mu\text{m}$  tall pillar was transferred to a PMMA sheet by nanoimprinting using the Ni mold fabricated from AR-P 3250. The sidewall of the pillar is as smooth as the original resist structure obtained via PBW. AR 300-12 mixed with AR-P 3250 achieves thinner resist layers, capable of realizing much higher resolution compared with AR-P 3250; i.e. 120 nm wide structures in a 280 nm thick layer with 1 MeV proton has been obtained. The structures were also accurately transferred to Ni as the resist can easily be removed in acetone. Nanoimprinting was carried out with this Ni mold and 120 nm wide lines were replicated in spincoated PMMA layers. Much higher resolution was achieved with 1 MeV proton in ma-N 2401 i.e. 60 nm wide lines in 100 nm thick ma-N were realized. However, after electroplating, resist was stuck in Ni. Ni mold fabricated with ma-N 2410 featuring 500 nm wide and 1  $\mu\text{m}$  deep channel was tested in injection molding showing accurate transfer into plastic PMMA.

**Acknowledgments** We acknowledge the financial support from US air force, Japan office and MOE Singapore (R-144-000-312-112). We also acknowledge Dr. Zhao Jianhong's help with injection molding.

#### References

- Adesida I (1985) Fine line lithography using ion beams. *Nucl Instrum Methods Phys Res B* 7–8:923–928
- Ansari K, van Kan JA, Bettiol AA, Watt F (2004) Fabrication of high aspect ratio 100 nm metallic stamps for nanoimprint lithography using proton beam writing. *Appl Phys Lett* 85:476–478
- Biersack J, Haggmark LG (1980) A Monte Carlo computer program for the transport of energetic ions in amorphous targets. *Nucl Instrum Methods* 174:257–269
- Brenner KH, Frank M, Kufner M, Kufner S (1990) H<sup>+</sup> lithography for 3-D integration of optical circuits. *Appl Opt* 29(26)
- Dhima K, Steinberg C, Möllenbeck S, Mayer A, Scheer HC (2011) Thermal nanoimprint (T-NIL) with photoresists for hybrid lithography. *Proc SPIE* 7985:798506-1
- Dutta RK, van Kan JA, Bettiol AA, Watt F (2007) Polymer microlens replication by nanoimprint lithography using proton beam fabricated Ni stamp. *Nucl Instrum Methods Phys Res B* 260:464–467
- Gonin Y, Munnik F, Benninger F, Dias F, Mikhaïlov S (2004) *J Vac Sci Technol B* 22:1982
- Lee H-S, Yang H-H, Ra S, Yoon J-B (2011) Fabrication of a large-scale Ni stamp using a multi-level SU-8 photoresist mold for advanced printed circuit board. *J Micromech Microeng* 21:065026
- Liu Fan, Boon Tan Kheng, Malar P, bikkarolla SK, van Kan JA (2013) Fabrication of nickel molds using proton beam writing for micro/nano fluidic devices. *Microelectron Eng* 102:36–39
- Liu NN, Shao P, Kulkarni SR, Zhao JH, and van Kan JA (2010) Nickel injection mould fabrication via proton beam writing and UV lithography. *Key Eng Mater* 447–448:188–192
- Malar P, Jianhong Zhao, van Kan JA (2012) Fabrication of metallic stamps for injection moulding applications by combining proton beam writing and UV lithography. *Appl Surf Sci* 258: 4191–4194

- Menzel F, Spemann D, Petriconi S, Lenzner J, Butz T (2007) Proton beam writing of microstructures at the ion nanoprobe LIPSION. *Nucl Instrum Methods Phys Res B* 260:419
- Mistry P, Gomez MI, Smith RC, Thomson D, Grime GW, Webb RP, Gwilliam R, Jeynes C, Cansell A, Merchant M, Kirkby KJ (2007) Maskless proton beam writing in gallium arsenide. *Nucl Instrum Methods Phys Res B* 260:437–441
- Oh SH, Cho SU, Kim CS, Han YG, Cho C-S, Jeong MY (2011) Fabrication of nickel stamp with improved sidewall roughness for optical devices. *Microelectron Eng* 88:2900–2907
- Rajta I, Gomez MI, Abraham MH, Kiss ÁZ (2003) Proton beam micromachining on PMMA, Foturan and CR-39 materials. *Nucl Instrum Methods Phys Res B* 210:260–265
- Rajta I, Baradács E, Bettiol AA, Csige I, Tőkési K, Budai L, Kiss ÁZ (2005) Optimization of particle fluence in micromachining of CR-39. *Nucl Instrum Methods Phys Res B* 231:384–388
- Rajta I, Chatzichristidi M, Baradács E, cserhádi C, Raptis I, Manoli K, Valamontes ES (2007) Proton beam micromachined buried microchannels in negative tone resist materials. *Nucl Instrum Methods Phys Res B* 260:414
- Simcic J, Pelicon P, Rupnik Z, Mihelic M, Razzpet A, Jenko D, Macek M (2005) 3D micromachining of SU-8 polymer with proton microbeam. *Nucl Instrum Methods Phys Res B* 241:479
- Springham SV, Osipowicz T, Sanchez JL, Gan LH, Watt F (1997) Micromachining using deep ion beam lithography. *Nucl Instrum Methods Phys Res B* 130:155–159
- Teo EJ, Liu MH, Breese MBH, Tavernier EP, Bettiol AA, Blackwood DJ, Watt F (2004) Fabrication of silicon microstructures using a high-energy ion beam. In: *Proceeding of SPIE 5347, Micromachining Technology for Micro-Optics and Nano-Optics II*, p 264
- Udalagama CNB, Bettiol AA, Watt F (2007) A Monte Carlo study of the extent of proximity effects in e-beam and p-beam writing of PMMA. *Nucl Instrum Methods Phys Res B* 260:384–389
- Valamontes E, Chatzichristidi M, Tsikrikas N, Goustouridis D, Raptis I, Potiriadis C, van Kan JA, Watt F (2008) Realization and simulation of high-aspect-ratio micro/nanostructures by proton beam writing. *Jpn J Appl Phys* 47:8600–8605
- van Kan JA, Sanchez JL, Xu B, Osipowicz T, Watt F (1999) Resist materials for proton micromachining. *Nucl Instrum Methods Phys Res B* 158:179–184
- van Kan JA, Sum TC, Osipowicz T, Watt F (2000) Sub 100 nm proton beam micromachining: theoretical calculations on resolution limits. *Nucl Instrum Methods Phys Res B* 161:366–370
- van Kan JA, Bettiol AA, Watt F (2003) Three dimensional nanolithography using proton beam writing. *Appl Phys Lett* 83(8):1629
- van Kan JA, Bettiol AA, Watt F (2006) Proton beam writing of 3D nanostructures in hydrogen SilsesQuioxane. *Nano Lett* 6:579–582
- van Kan JA, Bettiol AA, Chiam SY, Saifullah MSM, Subramanian KRV, Welland ME, Watt F (2007) New resists for proton beam writing. *Nucl Instrum Methods Phys Res B* 260:460–463
- van Kan JA, Zhang F, Chiam SY, Osipowicz T, Bettiol AA, Watt F (2008) Proton beam writing: a platform technology for nanowire production. *Microsyst Technol* 14:1343
- van Kan JA, Shao PG, Wang YH, Malar P (2011) Proton beam writing a platform technology for high quality three dimensional metal mold fabrication for nanofluidic applications. *Microsyst Technol* 17:1519–1527
- van Kan JA, Malar P, de Vera Armin Baysic (2012) The second generation Singapore high resolution proton beam writing facility. *Rev Sci Instrum* 83:902
- Voigt A, Elsner H, Meyer GH, Gruetzner G (1999) Nanometer patterning using ma-N 2400 series DUV negative photoresist and electron beam lithography. *SPIE* 3676:485
- Wang YH, Malar P, Zhao J, van Kan JA (2013) Resist evaluation for Ni mold fabrication and proton beam writing. *Microelectron Eng* 102:40–43
- Watt F, van Kan JA, Rajta I, Bettiol AA, Choo TF, Breese MBH, Osipowicz T (2003) The National University of Singapore high energy ion nano-probe facility: performance tests. *Nucl Instrum Methods Phys Res B* 210:14–20
- Yao Y, Santhana Raman P, van Kan JA (2014) Orthogonal and fine lithographic structures attained from the next generation proton beam writing facility. *Microsyst Technol*. doi:10.1007/s00542-014-2066-2
- Ynsa MD, Shao P, Kulkarni SR, Liu NN, van Kan JA (2011) Exposure parameters in proton beam writing for KMPR and EPO Core negative tone photoresists. *Nucl Instrum Methods Phys Res B* 269:2409–2412
- Zheng Cui (2005) *Micro-nanofabrication technologies and applications*. Springer, New York
- Ziegler JF (1999) The stopping of energetic light ions in elemental mater. *J Appl Phys* 85:1249–1272